

SEGMENTATION AND SHAPE TRACKING OF WHOLE FLUORESCENT CELLS BASED ON WAVELET OTSU MODEL

Mrs. D. Jagadiswary (Asso.Professor)
Dr .Pauls Engineering College
Mail id:jagadiswarypec@gmail.com

Ms. V. Vijayalakshmi (PG Scholar)
Dr. Pauls Engineering College
Mail id: vijayalakshmi@mmani@gmail.com

Abstract- The ability of cells to exert forces on their environment and alter their shape as they move is essential to various biological processes such as the immune response, embryonic development, or tumorigenesis. For that we present a fast and robust approach to tracking the evolving shape of whole fluorescent cells in time-lapse series. To ensure efficiency, consistency, and completeness in data processing and analysis, computational tools are essential. The proposed tracking scheme allow simultaneous tracking of multiple cells over time, both frameworks have been integrated with a topological prior exploiting the object indication function. To perform simultaneous tracking two steps are improved. First, coherence-enhancing diffusion filtering is applied on each frame to reduce the amount of noise and enhance flow-like structures. Second, the cell boundaries are detected by minimizing the Chan-Vese model in the fast level set-like and graph cut frameworks. The potential, advantages and disadvantages of both frameworks are demonstrated on proposed tracking scheme of 2D and 3D time-lapse series of rat adipose-derived mesenchymal stem cells and human lung squamous cell carcinoma cells, respectively.

I. INTRODUCTION

The important challenge in biomedical research understands the mechanisms of cell motility and their regulation. The crucial tasks are, in particular, segmenting, tracking, and evaluating movement tracks and morphological changes of cells, subcellular components, and other particles.

The typical fluorescence microscopy time-lapse series contain cells with significant spatio-temporal changes in intensity levels due to nonhomogeneous staining, uneven illumination, and photo bleaching.

To ensure efficiency, consistency, and completeness in data processing and analysis, computational tools are essential. Of particular importance to many modern live-cell imaging experiments is the ability to automatically track and analyze the motion of objects in time-lapse microscopy images.

Although cell motility and intracellular flows can be analyzed using optic flow or image registration techniques, the scope of this paper aims at identifying the boundaries of individual cells in each frame and tracking their evolution over time. Approaches developed for this specific task can broadly be classified as either tracking by detection or tracking by model evolution.

Understanding cell lineage relationships is fundamental to understanding development, and can shed light on disease etiology and progression. We present a method for automated construction of lineages of proliferative, migrating cells from a sequence of images.

Cell tracking over time has been one of the most revealing types of study for understanding developmental mechanisms. Normal progenitor cells undergo complex processes, including cell division, migration, changes in morphology, and death that are critical for tissue formation.

In contrast, the automated method is rapid and easily applied, and produces a wealth of measurements including the precise position, shape, cell-cell contacts, motility and ancestry of each cell in every frame, and accurate timings of critical events, e.g., mitosis and cell death. Furthermore, it automatically produces graphical output that is immediately accessible.

The tracking by detection approach is well-suited to experiments with low cell density, for which it is easy to determine the exact number of interacting cells in the current frame. Never-theless, with increasing cell density, the temporal association step often requires sophisticated strategies to deal with one-to-many and many-to-one matching problems effectively.

The minimization of original Chan-Vese model in the fast level set-like (FLS) and graph cut (GC) frameworks without solving any PDE, and replace coupling of multiple separate models with a topological prior that exploits the object indication function to allow simultaneous tracking of multiple cells over time.

Furthermore, to reduce the amount of noise in the acquired image data, increase the contrast along the cell boundaries, and enhance slender fiber-like structures often connecting individual regions of the cell cytoplasm, the tracking step is preceded by coherence-enhancing diffusion filtering (CED)

II. CHAN-VESE MINIMIZATION MODEL

The Chan-Vese model is a piecewise constant approximation to the functional formulation of image segmentation. This section recalls shortly the theoretical background and formulation of the Chan-Vese model

and the basic principles of the state-of-the-art frameworks developed for its minimization.

Its aim is to partition an input scalar image $u_0: \Omega \rightarrow \mathbb{R}$ defined over d -dimensional image domain $\Omega \rightarrow \mathbb{R}^d$ into two possibly disconnected regions Ω_1 (foreground) and Ω_2 (background) of low intra-region variance and separated by a smooth closed contour C ($\Omega = \Omega_1 \cup \Omega_2 \cup C$).

It can be formulated as,

$$E_{CV}(C, c_1, c_2) = \mu|C| + \lambda_1 \int_{\Omega_1} (u_0(x) - c_1)^2 dx + \lambda_2 \int_{\Omega_2} (u_0(x) - c_2)^2 dx$$

→ equation (1)

where c_1 and c_2 denote the unknown average intensity levels inside Ω_1 and Ω_2 , respectively, and μ , λ_1 and λ_2 are positive, user-defined weights.

Although the first two approaches represent the contour C differently, they are both based on a force-driven evolution of an initial contour. The explicit active contours are generally faster than level sets due to their light parametric representation of the contour C . However, their topological rigidity rules out the detection of multiple isolated objects from a single initial contour unless special surgical routines are used.

The minimization of the Chan-Vese model in the graph cut framework is more straightforward than in the previous ones. It is based on the fact that for fixed c_1 and c_2 it is possible to construct a graph G in which the cost of every cut approximates the energy of the corresponding segmentation from equation (1).

Therefore, a minimum cut of the graph G corresponds to a global minimum of equation (1) for fixed c_1 and c_2 . Subsequently, these values are updated according to the minimum cut and the computation is repeated until they reach a steady state.

In contrast to the previous frameworks, graph cuts do not require any initial contour to be specified. They only need some initial estimates of c_1 and c_2 . However, discrete graph cuts suffer from metrication errors and produce angular boundaries.

The denser the neighborhood system is when constructing the graph G , the smoother are the obtained boundaries. Unfortunately, increasing neighborhood density results in higher memory consumption, which could be critical, in particular, when processing large volumetric images.

III. INPUT IMAGE DATA

This section introduces two different time-lapse datasets of GFP-transfected cells analyzed for my experiments. All images were acquired using spinning-disk confocal microscopes. A summary of the cell types, acquisition setups, and image data properties is given in Table I. Sample frames from each of the datasets are shown in Fig. 1.

TABLE I

Cell Type, Acquisition Setup, And Properties Of Two Time-Lapse Datasets Analyzed In My Experiments

	Dataset 1	Dataset 2
Cell type	ADMSC	H157
Imaging system	Zeiss Cell Observer	PerkinElmer Ultraview ERS
Objective lens	Plan-Apo 20 X/0.85	Plan-Apo 63 X/1.20 Water
Frame size (vox)	512 X 478	580 X 540 X 60 (40; 35)
Voxel size (nm)	650 X 650	125:7 X 125:7 X 500:0
Time step (min)	5	1 (2)
No. of frames	19	20
No. of series	5	3 (4)

The first dataset consisted of five 2D time-lapse series of rat adipose-derived mesenchymal stem cells suspended in Minimum Essential Medium, which was supplemented with 10% Fetal Calf Serum and 1% Penicillin/Streptomycin, and monitored in a mixture of 1g=L collagen and 0:25% agarose poured on confocal Glass Bottom Microwell Dishes.

Each 2D time-lapse series had 19 frames captured every five minutes. The acquired 16-bit image data was compensated for uneven illumination by applying a flat-field correction procedure.

The second dataset consisted of seven 3D time-lapse series of human lung squamous cell carcinoma cells suspended in a 1:1 mixture of Matrigel/Collagen.

Each 3D time-lapse series had 20 frames that were captured every minute (three time-lapse series) or two (four time-lapse series). The acquired 16-bit image data contained one or two cells, 11 cells in total, having slightly heterogeneous cytoplasm of different intensity

levels.

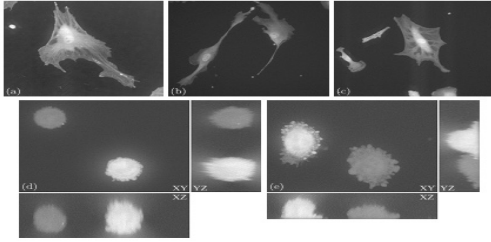


Fig. 1. Examples of analyzed input image data. (a)-(c) Three frames of different ADMSCs. (d) Maximum intensity projections along each axis of H157 cells poured on a confocal glass bottom microwell. (e) Maximum intensity projections along each axis of H157 cells injected in a growth medium.

BLOCK DIAGRAM:

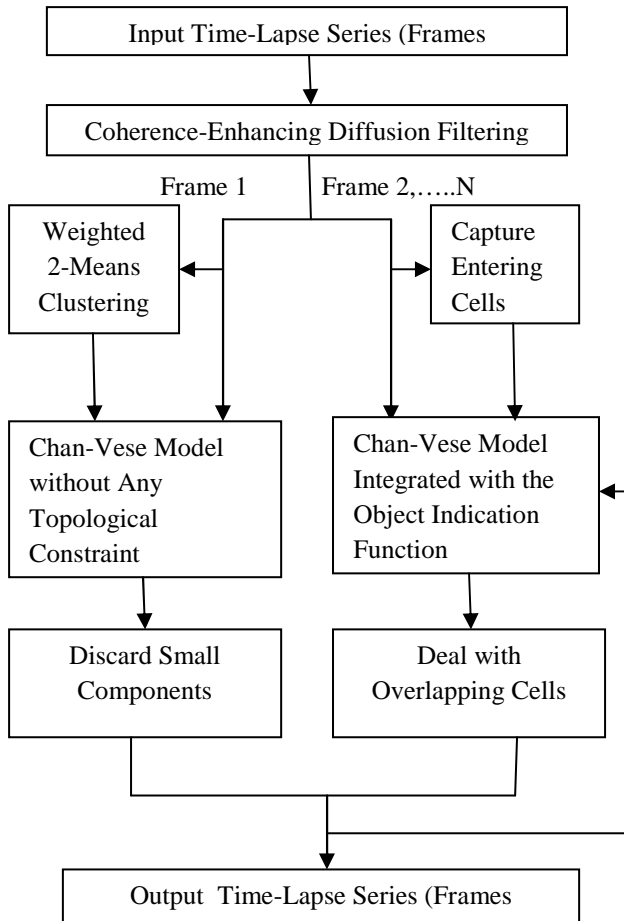


Fig. 2. Workflow of the proposed tracking scheme. The dashed line indicates using of a final result for the current frame as an additional information for the Chan-Vese model minimization routines when processing the next frame.

IV. PROPOSED TRACKING SCHEME

First, a coherence- enhancing diffusion filter is applied on each frame to reduce the amount of noise

and enhance flow-like structures. Second, the cell boundaries are detected by minimizing the Chan-Vese model in the FLS and GC frameworks. The initial models established for the cells detected in the first frame are evolved in time to fit the corresponding cells in the subsequent frames.

A. Coherence-Enhancing Diffusion Filtering

The completion of interrupted lines or the enhancement of flow-like structures is a challenging task in computer vision, human vision, and image processing. We address this problem by presenting a multiscale method in which a nonlinear diffusion filter is steered by the so-called interest operator (second-moment matrix, structure tensor).

An m-dimensional formulation of this method is analysed with respect to its well-posedness and scale-space properties. An efficient scheme is presented which uses a stabilization by a semi-implicit additive operator splitting (AOS), and the scale-space behaviour of this method is illustrated by applying it to both 2-D and 3-D images.

B. First Frame Segmentation

The FLS framework takes the final contour provided by the clustering, whereas graph cuts start with the corresponding foreground and background statistics. Once a steady state is reached, small components enclosing foreign particles such as dust are discarded from the final binary mask.

C. Capturing Entering Cells

New cells entering the field of view must be paid special attention. They have not been detected in the previous frames and are, therefore, considered part of the image background. This can affect significantly the background statistics and lead to incorrect segmentation of a particular frame.

F. Stopping Criterion

Specifically, the stopping criterion for the FLS framework is based on the detection of an oscillatory cycle. Let Δ^i denote the sum $|c_1^{i+1} - c_1^i| + |c_2^{i+2} - c_2^i|$ for two successive iterations i and $i+1$, $i \geq 0$. Let the counter C approach a cell boundary (i.e., a local minimum) in iteration $k \geq 0$. The counter C oscillates iff

$$|\Delta^{k+1} - \Delta^k| = 0 \quad \rightarrow \text{equation (2)}$$

For simplicity, let $\mu = 0$ and $\lambda_1 = \lambda_2 = 1$, thus an interface point $x \in \Omega$ is locally propagated inside or outside the contour C depending on the sign of the speed function $F : \Omega \rightarrow \mathbb{R}$, given as

$$F(x) = (f(x) - c_2)^2 - (f(x) - c_1)^2 \quad \rightarrow \text{equation (3)}$$

V. EXPERIMENTAL RESULTS

The experimental evaluation of the proposed tracking scheme conducted on a common workstation. We focus first on the optimal parameter settings for each framework. Then, we compare thoroughly their accuracy, execution time, and memory consumption.

A. Parameter Settings

The proposed tracking scheme has nine parameters that influence its overall performance. They can be divided into three groups according to their meaning and purpose. First, the parameters sr and wo reflect quantitative properties of tracked cells. They can be easily derived from the visual inspection of analyzed time-lapse series.

The parameter sr was fixed at 400 and 24 000 grid points in 2D and 3D, respectively. These values corresponded roughly to 20% of the minimum average size of a complete cell (i.e., a cell not touching the image border in the first frame) and allowed us to detect and track cells that appear only partly in the field of view.

B. Accuracy

In order to quantify the difference between the results of the tested methods, the Hausdorff distance H , given as

$$H(X, Y) = \max \left\{ \max_{x \in X} \min_{y \in Y} d_e(x, y), \max_{y \in Y} \min_{x \in X} d_e(y, x) \right\}$$

→ equation (4)

Generalizing the Euclidean distance d_e on two sets of grid points (segmentation results) X and Y was measured for each pair of them. Note that the measurements were no longer restricted only to 140 randomly chosen slices in 3D, but performed on complete 3D stacks.

VI. CONCLUSION

The proposed tracking scheme combines CED filtering with the FLS and GC frameworks that minimize the Chan-Vese model. It allows simultaneous tracking of multiple cells over time by applying a topological prior that exploits the object indication function. The experimental evaluation was performed on 2D and 3D time-lapse series of rat adipose-derived mesenchymal stem cells and human squamous cell carcinoma cells, respectively. This complicates the use of the proposed tracking scheme in experiments with high density of tightly packed cells. Furthermore, coherence-enhancing diffusion filtering takes up to about 85% of the total execution time. Therefore, a different choice of the filtering technique would make the proposed tracking scheme significantly faster and more suitable for high-throughput applications.

REFERENCES

- [1] C. Zimmer, B. Zhang, A. Dufour, A. Th'ebaud, S. Berlemont, V. Meas-Yedid, and J.-C. Olivo-Marin, "On the digital trail of mobile cells," *IEEE Signal Processing Magazine*, vol. 23, no. 3, pp. 54–62, 2006.
- [2] R. Ananthakrishnan and A. Ehrlicher, "The forces behind cell movement," *International Journal of Biological Sciences*, vol. 3, no. 5, pp. 303–317, 2007.
- [3] R. Fern'andez-Gonz'alez, A. Mu'noz-Barrutia, M. H. Barcellos-Hof, and C. Ortiz-de-Sol'orzano, "Quantitative in vivo microscopy: the return from the 'omics'," *Current Opinion in Biotechnology*, vol. 17, no. 5, pp. 501–510, 2006.
- [4] C. Vonesch, F. Aguet, J.-L. Vonesch, and M. Unser, "The colored revolution of bioimaging," *IEEE Signal Processing Magazine*, vol. 23, no. 3, pp. 20–31, 2006.
- [5] E. Meijering, O. Dzyubachyk, I. Smal, and W. A. Cappellen, "Tracking in cell and developmental biology," vol. 20, no. 8, pp. 894–902, 2009.